Available online at www.sciencedirect.com

ScienceDirect

Mendeleev Commun., 2018, **28**, 666–667

Mendeleev Communications

The possibility of electrochemical lithium intercalation into a nanodiamond

Dmitry Yu. Gryzlov, Tatiana L. Kulova, Alexander E. Alexenko, Boris V. Spitsyn and Alexander M. Skundin*

A. N. Frumkin Institute of Physical Chemistry and Electrochemistry, Russian Academy of Sciences, 119071 Moscow, Russian Federation. E-mail: askundin@mail.ru

DOI: 10.1016/j.mencom.2018.11.037

The principal possibility to intercalate lithium into a nanodiamond has been for the first time revealed.

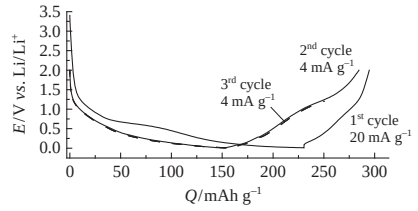

It is well known that lithium intercalates into graphite and non-graphitic (amorphous) carbon forms possessing layered structures, but cannot apparently intercalate into the well crystallized diamond. However, there is no *a priori* negative answer to the question whether lithium can be or not intercalated into the nanodiamond samples due to the imperfection of their structure. It has been experimentally shown[1,2] that lithium is intercalated into various nanodiamond composites with non-diamond forms of carbon, but only into the non-diamond phases. Lithium can still be implanted into diamond by one or another method, but it remains non-diffusible.[3–6] We are the first to report on the possibility of reversible lithium insertion into the diamond phase of composites containing the non-diamond carbon.

Two types of nanodiamond were used in this work: (1) commercial diamond powder of ASM grade with grain size no greater than 500 nm and (2) diamond films grown on silicon supports and then powdered.† Qualitatively identical results were obtained for the powders of both types.

It was shown by Raman spectroscopy that all the materials studied were composed of nearly pure diamond containing minor admixtures of non-diamond carbon. The Raman spectrum of diamond powder contained a sharp peak at 1332 cm^{-1} corresponding to the pure diamond[7–9] and a more diffuse peak in the region of 1500–1700 cm^{-1} corresponding to sp^2-carbon (Figure 1). Since the sensitivity of signal corresponding to the non-carbon diamond is *ca*. 50 times higher than that of diamond,[10] the content of non-diamond carbon in the test powders did not exceed fractions of a percent (see Figure 1).

Figure 2 shows the galvanostatic charge and discharge curves‡ recorded at various currents on electrodes containing the diamond

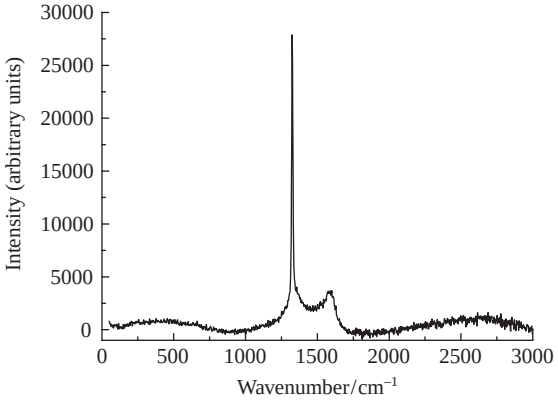

Figure 1 Raman spectrum of the diamond powder obtained from the grown diamond film.

† The size of single grains after grinding the films did not exceed 400 nm. The specific surface area of the powder determined by the BET method was *ca*. 800 $m^2\ g^{-1}$. The films were grown from a carbon-containing gas phase diluted with hydrogen and activated by non-self-maintained direct current discharge. The process was performed in a flow-through chamber at a pressure of about 0.1 atm, into which hydrogen pre-bubbled through a bulb containing a mixture of ethanol and boric acid was fed. As a result, the gaseous crystallization medium was a source of carbon and boron simultaneously. Thermal and electrical activation of the gas phase produced excited hydrocarbon molecules and simplest carborane molecules that can decompose on substrate surface heated to *ca*. 1000 °C to give the free carbon, predominantly in the form of diamond doped with boron, as well as atomic hydrogen that served as a selective etchant towards the nuclei of non-diamond carbon forms, thus preventing their further growth on the substrate. To simplify the formation of a new diamond phase on the foreign surface, a monolayer of powder particles of natural or synthetic diamond with sizes of about 1 μm was deposited on the surface. Using this method, the films of semiconductive p-type diamond were obtained, with thicknesses from few to few dozens of μm, containing up to 0.1 at% boron and possessing the minimum electric conductance of few dozens of Ohm between point contacts.

‡ The starting electrodes were prepared by pasting a mixture of diamond powder (90%) and binder (10%), *viz*., polyvinylidenefluoride (PVDF) dissolved in *N*-methylpyrrolidone, on a stainless steel mesh current-collector. After pasting, the electrodes were compressed under the pressure of 5 tons cm^{-2}, dried in order to remove the solvent, and heat treated at 900 °C *in vacuo*. Heat treatment resulted in PVDF carbonization to give an amorphous carbon phase whose content in the active material was ~4%.

Electrochemical measurements were performed in hermetically sealed three-electrode cells with a lithium auxiliary electrode and a lithium reference electrode. The cells were assembled and filled with the electrolyte in a glove box filled with dry argon. An 1 M $LiPF_6$ solution in an ethylene carbonate–diethyl carbonate–dimethyl carbonate mixture (1 : 1 : 1) was used as the electrolyte (all the electrolyte components were of extra dry grade and purchased from Aldrich). The water content in the electrolyte did not exceed 20 ppm. Nonwoven polypropylene of 25 μm thickness ('Ufim' Scientific Production Association, Russia) was used as the separator. Galvanostatic testing of the electrochemical cells was performed using a computer-controlled facility ('Booster' Closed Joint-Stock Company, Russia).

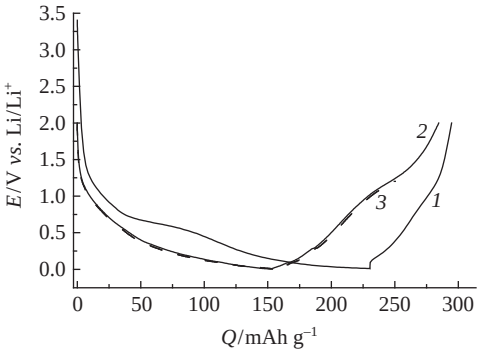

Figure 2 Galvanostatic charge and discharge curves at the currents of (*1*) 20 mA g^{-1} and (*2*), (*3*) 4 mA g^{-1}.

powder. At the first cycle performed at the current of 20 mA g^{-1}, a characteristic irreversible capacity is observed due to the electrolyte reduction and formation of a passive film (solid electrolyte interphase, SEI).[2] The second and third cycles were recorded at the current of 4 mA g^{-1}. One can see that these curves nearly coincide. Upon further cycling at 4 mA g^{-1}, the capacity degradation did not exceed 0.05% per cycle during 80 cycles, which is typical of the majority of electrodes.

As one can see from Figure 2, the anodic (discharge) capacity at the relatively low current (4 mA g^{-1}) amounts to 130 mAh g^{-1}, while at the current of 20 mA g^{-1}, it decreases to 63 mAh g^{-1}. Even taking into consideration that a fraction of discharge capacity is due to the presence of non-diamond carbon whose content is 4%, the diamond component still accounts for at least 115 mAh g^{-1}, which is clearly beyond the error. According to Faraday laws, the capacity of 115 mAh g^{-1} corresponds to an atomic concentration of intercalated lithium of 5×10^{21} cm^{-3}. The data on diffusion doping of diamond films with lithium from a lithium nitride (Li_3N) suspension to a concentration of 5×10^{19} cm^{-3} was reported.[3] In another work,[4] a concentration of 2×10^{20} cm^{-3} was obtained by the similar doping of diamond films alloyed with boron.

The mechanism of lithium intercalation into the diamond phase remains debatable. The shape of galvanostatic curves (see Figure 2) is typical of lithium intercalation into the non-graphitic carbon forms. It may be assumed that the lithium intercalation into diamond occurs one or another way related to the defectiveness of latter.[11] In principle, we cannot rule out lithium localization at inner interphase boundaries. Indeed, based on the facts that specific surface area of considered material accounts to 800 m^2 g^{-1} and lithium intercalation is close to 115 mAh g^{-1}, the lithium coverage of these interphase boundaries could be estimated as much as 3×10^{14} cm^{-2}. The known[12] natural limit of number of ions chemisorbed at the inner surface of nanodiamond with 5 nm particles was reported as 1.8×10^{15} cm^{-2}, which is in agreement with our results.

In the present work, we did not evaluate the change of lattice dimension during the lithium intercalation. With the well-known data on the graphite lithiation in mind, the volume expansion of nanodiamond at the maximal lithium intercalation could be estimated as *ca*. 5%. At the same time, we recognize the importance of this problem and suppose that such a study will be made in the future.

To conclude, we have for the first time demonstrated the practical possibility for the lithium intercalation into a nanodiamond, which is the promising opportunity for a design of new materials.

This study was performed within the framework of State Task for A. N. Frumkin Institute of Physical Chemistry and Electrochemistry of the Russian Academy of Sciences (project no. 47.23).

References

1 L.-F. Li, D. A. Totir, N. Vinokur, B. Miller, G. Chottiner, E. A. Evans, J. C. Angus and D. A. Scherson, *J. Electrochem. Soc*., 1998, **145**, L85.
2 T. L. Kulova, Yu. E. Evstefeeva, Yu. V. Pleskov, A. M. Skundin, V. G. Ral'chenko, S. B. Korchagina and S. K. Gordeev, *Phys. Solid State*, 2004, **46**, 726.
3 M. Zamir Othman, P. W. May, N. A. Fox and P. J. Heard, *Diamond Relat. Mater*., 2014, **44**, 1.
4 S. C. Halliwell, P. W. May, N. A. Fox and M. Z. Othman, *Diamond Relat. Mater*., 2017, **76**, 115.
5 R. A. Khmelnitsky, V. V. Saraykin, V. A. Dravin, E. V. Zavedeyev, S. V. Makarov, V. S. Bronsky and A. A. Gippius, *Surf. Coat. Technol*., 2016, **307**, 236.
6 J. te Nijenhuis, G. Z. Cao, P. C. H. J. Smits, W. J. P. van Enckevort, L. J. Giling, P. F. A. Alkemade, M. Nesládek and Z. Remeš, *Diamond Relat. Mater*., 1997, **6**, 1726.
7 C. Ramaswamy, *Nature*, 1930, **125**, 704.
8 S. A. Solin and A. K. Ramdas, *Phys. Rev. B*, 1970, **1**, 1687.
9 P. Bou and L. Vandenbulcke, *J. Electrochem. Soc*., 1991, **138**, 2991.
10 R. J. Nemanich, J. T. Glass, G. Lucovsky and R. E. Shroder, *J. Vac. Sci. Technol. A*, 1988, **6**, 1783.
11 K. Kobashi, *Diamond Films: Chemical Vapor Deposition for Oriented and Heteroepitaxial Growth*, Elsevier, Amsterdam, 2005.
12 V. Yu. Osipov, I. D. Gridnev and A. M. Panich, *Mendeleev Commun*., 2018, **28**, 404.

Received: 11th April 2018; Com. 18/5540